M(III). The inductive effect is a major contributor even in significantly delocalized systems like the Creutz-Taube ion,[27,30] so it is expected to be important in less delocalized systems as well.

There is also a stabilization to the mixed-valence state due to simple electrostatic repulsion of the two metal centers, which for the pentaammineruthenium systems gives a slight advantage to the mixed-valence vs. isovalent forms. A calculation based on the Fuoss approach to ion pairing[32-34]

$$\Delta G_A = \frac{z_1 z_2 e_0^2}{D_S d} \frac{1}{1 + \kappa d} - RT \ln \frac{4Nd^3}{3000}$$

where z_1, z_2 = charge on monometallic fragments, $e_0^2 = 3.318 \times 10^{-3}$ cal cm/mol, D_S = dielectric constant (80 for 0.1 M ionic strength H_2O at 23 °C),[32] d = intermetallic separation, κ = Debye inverse length ($(0.329 \times 10^8) I^{1/2}$ cm^{-1} for H_2O at 23 °C), N = Avogadro's number, and R = 1.987 cal/(mol K), and Hess's law

$$\Delta G_{MV} = 2G_A(\text{Fe(II),Fe(III)}) - [G_A(\text{Fe(II),Fe(II)}) + \Delta G_A(\text{Fe(III),Fe(III)})]$$

yields ΔG_{MV}(bpm) = −294 cal/mol and ΔG_{MV}(dpp) = −184 cal/mol. While the simplistic nature of this model underestimated ΔG_{MV},[27] the result is consistent with the expectation that the smaller metal-metal separation should yield a greater electrostatic stabilization of the mixed-valence form. The fact that the electrostatic stabilization for bpm is greater than for dpp, in spite of the fact that overall the mixed-valence-state dpp-bridged system is more stable than the bpm-bridged complex, focuses attention on the remaining contribution to mixed-valence stabilization, electronic delocalization.

Richardson and Taube[29] have noted that if a metal is bound to a starred position of an alternating hydrocarbon, the strongest metal-metal interaction is observed if the second metal is bound to an unstarred position. This is based on general observation of the transmission of electronic effects through conjugated bond systems, as well as by mechanistic theories.[29] If the star formalism is applied to bpm and dpp, the following results:

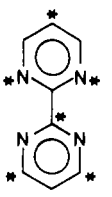
bpm

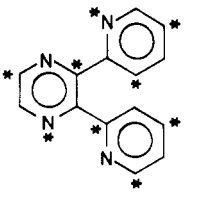
dpp

This suggests that the electronic distribution for dpp (a 1,4-coordination on the pyrazine ring) is more favorable for metal-metal interaction than in bpm (a 1,3-coordination on each pyrimidine ring). A more quantitative estimate of the extent of electronic interaction can be made from intervalence transfer band data, which are currently under investigation.[25]

Conclusion

From the $E_{1/2}$ values we can see that dpp functions well as a bridging ligand and provides excellent communication between the two metal centers. The dpp ligand provides a means to separate the metal centers, thereby reducing steric crowding.

These bimetallic systems show that we can bridge two first-row transition-metal centers using either bpm or dpp as the bridging ligand. The electrochemical data seem to indicate a large amount of communication between the metal centers, supporting our idea of possible energy transfer across the bridging ligand. The results presented here indicate that dpp may yield more promising results than bpm in the preparation of mixed-metal bimetallic complexes since it significantly lowers the steric crowding without reducing the communication between the metal centers.

Acknowledgment. We thank the Office of Basic Energy Science, Department of Energy (Contract No. DE-AS09-80ER10671), for support of this research.

Registry No. $K_2[Fe(CN)_4(bpm)]$, 92787-94-5; $K_4[Fe(CN)_4]_2(bpm)$, 109765-39-1; $K_2[Fe(CN)_4(dpp)]$, 109765-40-4; $K_4[Fe(CN)_4]_2(dpp)$, 109765-41-5; $Fe(CN)_4(bpm)^-$, 109765-42-6; $[Fe(CN)_4]_2(bpm)^{3-}$, 109765-43-7; $[Fe(CN)_4]_2(bpm)^{2-}$, 97823-73-9; $Fe(CN)_4(dpp)^-$, 109765-44-8; $[Fe(CN)_4]_2(dpp)^{3-}$, 109765-45-9; $[Fe(CN)_4]_2(dpp)^{2-}$, 109765-46-0.

(32) Sutton, J. E.; Sutton, P. M.; Taube, H. *Inorg. Chem.* **1979**, *18*, 1017.
(33) Curtis, J. C.; Sullivan, B. P.; Meyer, T. J. *Inorg. Chem.* **1980**, *19*, 3833.
(34) Fuoss, R. M. *J. Am. Chem. Soc.* **1958**, *80*, 5059.

Contribution from the Chemical Crystallography Laboratory, University of Oxford, Oxford OX1 3PD, U.K., and Central Research and Development Department,[1] E. I. du Pont de Nemours and Company, Experimental Station, Wilmington, Delaware 19898

Preparation, Structure, and Magnetic Properties of a New Form of Chromium Orthoarsenate: β-$CrAsO_4$

J. Paul Attfield,*[2a] Anthony K. Cheetham,[2a] David C. Johnson,[2b,c] and Charlie C. Torardi*[2b]

Received February 17, 1987

A new (β) form of $CrAsO_4$ has been prepared at 700 °C under 3-kbar hydrothermal pressure, and a single-crystal X-ray study shows that β-$CrAsO_4$ adopts the $ZnSO_4$ structure (a = 8.995 (2) Å, b = 6.237 (3) Å, c = 4.755 (1) Å, Z = 4, space group *Pnma*). The ordered magnetic structure at 5 K has been determined from a powder neutron diffraction experiment and consists of Cr^{3+} moments of 2.38 (4) μ_B parallel to c, antiferromagnetically ordered both in the ac plane and along b. Variable-field magnetic susceptibility measurements are consistent with antiferromagnetic behavior in the high-temperature Curie-Weiss limit but reveal ferrimagnetic behavior below the Néel temperature of 10 ± 2 K. This is consistent with magnetic symmetry arguments that show that a weak field-induced ferromagnetic component parallel to b is allowed. This magnetic behavior is compared with that of other $ZnSO_4$ type materials.

Introduction

Crystalline salts of the first-row transition metals have been of interest for many years in the study of the magnetic behavior of the various $3d^n$ electronic configurations and the interactions between the magnetic ions. As part of this effort, the low-temperature magnetic properties and ordered magnetic structures of many salts with the $CrVO_4$[3] or the related $ZnSO_4$[4] structure have been studied. Both of these orthorhombic structures consist of infinite chains of trans edge-sharing MO_6 octahedra, with XO_4 tetrahedra linking the chains. Strong ferromagnetic or antifer-

(1) Contribution No. 4307.
(2) (a) University of Oxford. (b) E. I. du Pont de Nemours and Co. (c) Current address: Department of Chemistry, University of Oregon, Eugene, OR 97403.
(3) Frazer, B. C.; Brown, P. J. *Phys. Rev.* **1962**, *125*, 1283.
(4) Kokkoros, P. A.; Rentzperis, P. J. *Acta Crystallogr.* **1958**, *11*, 361.

0020-1669/87/1326-3379$01.50/0

Table I. Summary of Single-Crystal Data Collection and Refinement for β-$CrAsO_4$

cryst color	light green
cryst dimens, mm	0.01 × 0.04 × 0.37
radiatn	Mo Kα
monochromator	graphite
cryst syst	orthorhombic
space group	*Pnma*
cell dimens, Å	a = 8.955 (2)
	b = 6.237 (3)
	c = 4.755 (1)
calcd density, g cm^{-3}	4.77
scan mode	ω
2θ range, deg	0–55
octants	*HKL*, $\bar{H}KL$
μ, cm^{-1}	163.7
transm coeff range	0.57–0.79
no. of tot obsd reflcns	729
no. of indep reflcns ($I > 2\sigma$)	233
R	0.031
R_w[a]	0.033

[a] $R_w = [\sum w(|F_o| - |F_c|)^2 / \sum w|F_o|^2]^{1/2}$ with w proportional to $1/[\sigma^2(I) + (0.02I)^2]$.

romagnetic interactions along the chains are observed, in agreement with Kanamori's rules for 90° M–O–M exchange pathways,[5] but the ordering between chains is more complex and is not well understood. Several collinear or coplanar antiferromagnetic structures have been reported,[3,6-15] and two examples of incommensurate cycloidal spiral structures are also known in $CrVO_4$ type salts.[16,17] One of these, β-$CrPO_4$, has recently been shown to have a spiral of moments in the *ab* plane that propagates along the x axis with periodicity $\sim 3a$.[17] By contrast, $CrVO_4$ has a commensurate magnetic structure with spins lying close to the x axis.[3]

The only form of $CrAsO_4$ that has been previously reported[18] has the α-$CrPO_4$ sttructure,[19] which is unrelated to those described above in that it does not contain infinite chains of edge-sharing CrO_6 octahedra. We are currently investigating the magnetic properties and thermodynamic stability of α-$CrPO_4$ and α-$CrAsO_4$. Here we report the preparation of a $ZnSO_4$ type polymorph, β-$CrAsO_4$, and the magnetic structure and susceptibility variation of this new phase.

Experimental Section

Hydrothermal reaction of Cr_2O_3 with a solution of H_3PO_4 in sealed gold tubes at 700 °C and 3-kbar pressure was found to give light green β-$CrAsO_4$ as the only product. Thermogravimetric analysis of this material confirmed the composition and showed that it is air stable to ~900 °C, above which it decomposes into Cr_2O_3 and volatile arsenic oxides. Slow cooling of a charge containing 1.0 g of Cr_2O_3 and 4 mL of 4.0 M H_3AsO_4 from 700 to 300 °C at 20 °C h^{-1} resulted in the formation of small needle-shaped crystals of the new phase. One of these was mounted on an Enraf-Nonius CAD 4 diffractometer for structure determination; details of the data collection are summarized in Table I.

A polycrystalline sample of β-$CrAsO_4$ was used for the magnetic measurements. Magnetic susceptibility data were obtained between 1.8 and 325 K at fields ranging from 5.5 to 19.5 kG by using a high-sensitivity Faraday balance. With a ~20-mg sample, the error in the calculated susceptibility is 0.5%. Neutron diffraction data were collected from ~10 g of β-$CrAsO_4$ held in a vanadium can in a cryostat at 5 K on diffractometer D1A at the ILL, Grenoble, France. The diffraction profile was recorded between 6 and 156° 2θ at a wavelength of 1.95 Å.

Table II. Refined Structural Parameters for β-$CrAsO_4$ in *Pnma* (No. 53): Fractional Coordinates and Isotropic Thermal Parameters from the Single-Crystal X-ray Structure Refinement and the 5 K Powder Neutron Rietveld Analysis (Marked N), with Esd's in Parentheses

atom	symm position	x	y	z	B_{iso}, Å^2[a]
Cr	4a	0	0	0	0.5 (0)
As	4c	0.1806 (1)	0.2500	0.4771 (2)	0.4 (0)
		0.1807 (2)^N		0.4784 (5)^N	
O(1)	4c	0.1153 (9)	0.2500	0.8150 (15)	0.6 (2)
		0.1135 (4)^N		0.8170 (5)^N	
O(2)	4c	0.3715 (9)	0.2500	0.4153 (15)	0.6 (2)
		0.3697 (4)^N		0.4150 (5)^N	
O(3)	8d	0.1244 (6)	0.0236 (9)	0.3273 (11)	0.6 (1)
		0.1254 (3)^N	0.0237 (3)^N	0.3289 (4)^N	

[a] Overall B_{iso} for the Rietveld refinement is 0.21 (3) Å^2.

Table III. Bond Distances (Å) and Angles (deg) for β-$CrAsO_4$ from the Single-Crystal X-ray Structure Refinement with Esd's in Parentheses

Distances and Angles

Cr–O(1)[d] (×2)	2.067 (5)	As–O(1)	1.710 (7)
Cr–O(2)[e] (×2)	1.979 (5)	As–O(2)	1.734 (8)
Cr–O(3) (×2)	1.919 (5)	As–O(3) (×2)	1.660 (5)
O(1)[d]–Cr–O(1)[f]	180.0	O(1)–As–O(2)	119.8 (4)
O(1)[d]–Cr–O(2)[g]	77.4 (2)	O(1)–As–O(3)	107.4 (2)
O(1)[d]–Cr–O(2)[e]	102.6 (2)	O(2)–As–O(3)	103.1 (2)
O(1)[d]–Cr–O(3)[h]	90.1 (3)	O(3)–As–O(3)[a]	116.6 (4)
O(1)[d]–Cr–O(3)	89.9 (3)	As–O(1)–Cr[b]	124.8 (2)
O(2)[e]–Cr–O(2)[g]	180.0	As–O(2)–Cr[i]	122.6 (2)
O(2)[e]–Cr–O(3)	83.6 (3)	As–O(3)–Cr	126.1 (3)
O(2)[e]–Cr–O(3)[h]	96.4 (3)	Cr[b]–O(1)–Cr[c]	98.0 (3)
O(3)[h]–Cr–O(3)	180.0	Cr[i]–O(2)–Cr[j]	104.0 (4)

Symmetry Operation Codes

a	$x, {}^1/_2 - y, z$	f	$-x, -y, 1 - z$
b	$x, y, 1 + z$	g	$-{}^1/_2 + x, y, {}^1/_2 - z$
c	$x, {}^1/_2 - y, 1 + z$	h	$-x, -y, -z$
d	$x, y, -1 + z$	i	${}^1/_2 - x, {}^1/_2 + y, {}^1/_2 + z$
e	${}^1/_2 - x, -{}^1/_2 + y, -{}^1/_2 + z$	j	${}^1/_2 + x, y, {}^1/_2 - z$

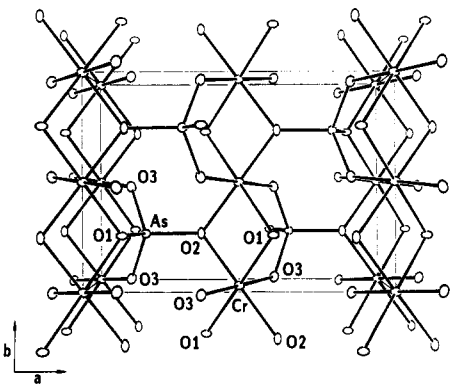

Figure 1. ORTEP perspective of the crystal structure of β-$CrAsO_4$ viewed down c.

Results

Crystal Structure.[20] The single-crystal X-ray diffraction data were collected at ambient temperature and corrected for Lorentz and polarizaton effects, and an empirical absorption correction

(5) Kanamori, J. *Phys. Chem. Solids* **1959**, *10*, 87.
(6) Bertaut, E. F.; Coing-Boyat, J.; Delapalme, A. *Phys. Lett.* **1963**, *3*, 178.
(7) Brown, P. J.; Frazer, B. C. *Phys. Rev.* **1963**, *129*, 1145.
(8) Almodovar, I.; Frazer, B. C.; Hurst, J. J.; Cox, D. E.; Brown, P. J. *Phys. Rev.* **1965**, *138*, A153.
(9) Fuess, H.; Will, G. *J. Appl. Phys.* **1968**, *39*, 628.
(10) Fuess, H. *Z. Angew. Phys.* **1969**, *27*, 311.
(11) Pernet, M.; Quezel, G.; Coing-Boyat, J.; Bertaut, E. F. *Bull. Soc. Fr. Mineral. Cristallogr.* **1969**, *92*, 264.
(12) Scharenberg, W.; Will, G. *J. Phys. (Les Ulis, Fr.)* **1971**, *32*, 851.
(13) Kirfel, A.; Will, G. *Int. J. Magn.* **1973**, *5*, 197.
(14) Kirfel, A.; Schafer, W.; Will, G.; Buschow, K. H. J. *Phys. Status Solidi A* **1977**, *40*, 447.
(15) Battle, P. D.; Gibb, T. C.; Hu, G.; Munro, D. C.; Attfield, J. P. *J. Solid State Chem.* **1986**, *65*, 343.
(16) Will, G.; Frazer, B. C.; Shirane, G.; Cox, D. E.; Brown, P. J. *Phys. Rev.* **1965**, *140*, A2139.
(17) Attfield, J. P.; Battle, P. D.; Cheetham, A. K. *J. Solid State Chem.* **1985**, *57*, 357.
(18) Ronis, M. M. *C. R. Seances Acad. Sci., Ser. C* **1970**, *271C*, 64.
(19) Attfield, J. P.; Sleight, A. W.; Cheetham, A. K. *Nature (London)* **1986**, *322*, 620.

(20) All X-ray crystallographic calculations were performed on a Digital Equipment Corp. VAX 11/780 computer using a system of programs developed by J. C. Calabrese.

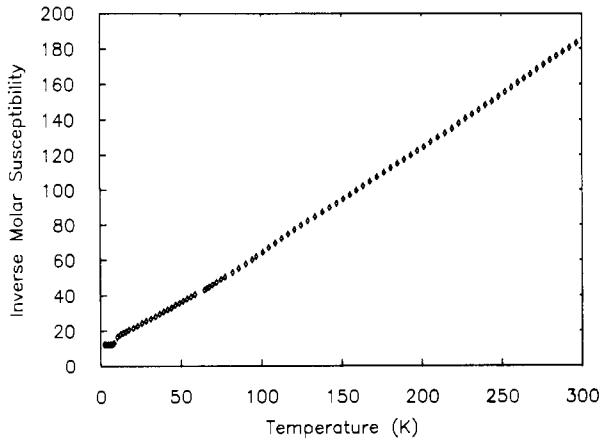

Figure 2. Inverse molar magnetic susceptibility of β-$CrAsO_4$ between 2 and 300 K.

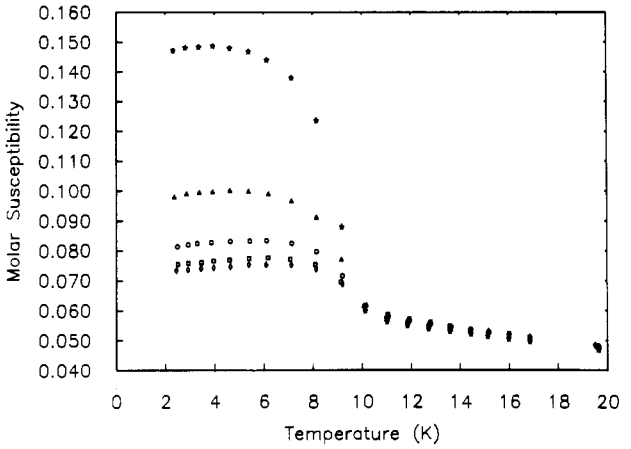

Figure 3. Low-temperature magnetic susceptibility data for β-$CrAsO_4$ measured at applied fields of 5.5 (stars), 11.0 (triangles), 15.7 (circles), 18.3 (squares), and 19.5 kG (diamonds).

(ψ-scan method) was applied. β-$CrAsO_4$ was found to have the $ZnSO_4$ structure, and the structural parameters of the latter[3] were taken as a starting model for a least-squares refinement of the positional and anisotropic thermal parameters in space group *Pnma*. Only reflections with $I > 2\sigma$ were used in the refinement, which converged successfully to $R = 0.031$ and $R_w = 0.033$, giving the refined values shown in Table II. Calculated bond distances and angles are displayed in Table III, and a view of the structure is shown in Figure 1.

Magnetic Susceptibility Measurements. The inverse magnetic susceptibility data (Figure 2) show a Curie–Weiss behavior at high temperatures. A linear fit using the data above 150 K gives a Curie–Weiss temperature of −16 K and an effective magnetic moment of 3.7 μ_B (the spin-only value is 3.87 μ_B). At low temperatures, the susceptibility data deviate from the Curie–Weiss curve due to the onset of magnetic ordering, and a broad susceptibility maximum is observed (see Figure 3). Increasing the applied field reduces this maximum and shifts the position to higher temperatures: from 4 K at 5.5 kG to 6 K at 19.5 kG. The ordering temperature T_N is identified with the region of maximum slope at 10 ± 2 K.

Neutron Diffraction. The nuclear contributions to the 5 K neutron diffraction data were fitted by the Rietveld method,[21] starting with the coordinates from the single-crystal structure determination. This revealed several magnetic peaks at low angles, all of which can be indexed upon the atomic unit cell. In determining the nature of the magnetic ordering, it is useful to consider the possible spin arrangements by using the notation of Bertaut.[22] With four magnetic ions in the unit cell, there are four base vectors arising from collinear combinations of the individual spins, which are shown in Table IV with the magnetic reflection conditions due to each one. One of these combinations (**F**) represents ferromagnetic ordering of the spins, and the rest are antiferromagnetic. All of the observed magnetic reflections have both $h + l$ and k taking odd values, corresponding to the antiferromagnetic **G** combination of moments. To determine the direction of the spins, several magnetic models were fitted to the profile. The only one to give a good fit to the magnetic peaks (magnetic R factor = 15.4%) was the one with the moment parallel to c, the refined value of the moment being 2.38 (4) μ_B. The expected, profile, and weighted profile R factors[23] for the refinement were 6.5%, 12.2%, and 11.9%, respectively, and a plot of observed, calculated, and difference intensities is shown in Figure 4, with magnetic peaks labeled. The atomic parameters obtained from the refinement are given in Table II for comparison with the X-ray values, and the refined cell parameters are a = 8.9433 (1) Å, b = 6.2190 (1) Å, and c = 4.7484 (1) Å. The magnetic structure is displayed in Figure 5.

Table IV. Four Base Vectors Arising from Different Spin Combinations in Space Group *Pnma* and Resulting Magnetic Reflection Conditions

base vector	spins[a]				reflcn conditions	
	S_1	S_2	S_3	S_4	$h + l$	k
F	+	+	+	+	even	even
G	+	−	+	−	odd	odd
C	+	+	−	−	odd	even
A	+	−	−	+	even	odd

[a] Spins S_1, S_2, S_3, and S_4 are at (0, 0, 0), (0, $^1/_2$, 0), ($^1/_2$, $^1/_2$, $^1/_2$), and ($^1/_2$, 0, $^1/_2$), respectively.

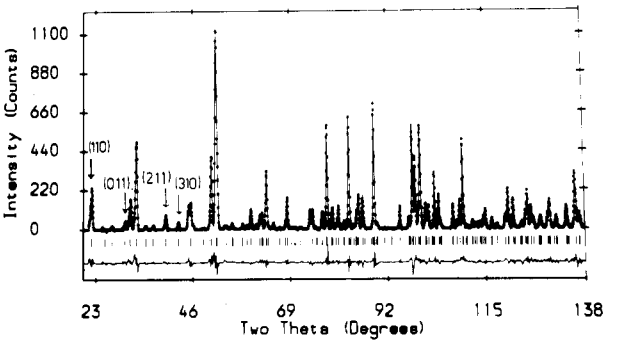

Figure 4. Observed (points), calculated (full line), and difference profiles for the powder neutron diffraction pattern of β-$CrAsO_4$ at 5 K. Reflection positions are marked, and magnetic diffraction peaks are labeled.

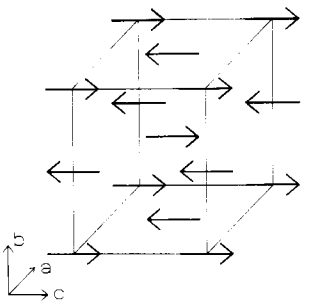

Figure 5. Antiferromagnetic structure of β-$CrAsO_4$ at 5 K determined from the neutron diffraction experiment.

Discussion

High-pressure β-$CrAsO_4$ is 14% denser than the α polymorph, which results from preparations at atmospheric pressure, and it seems to be indefinitely stable at room temperature and pressure.

(21) Rietveld, H. M. *J. Appl. Crystallogr.* **1969**, *2*, 65.

(22) Bertaut, E. F. In *Treatise on Magnetism*; Rado, G. T., Suhl, H., Eds.; Academic Press: New York, 1963; Vol. III, p 150.

(23) The R factors from the profile analysis are defined in ref 21.

Table V. Irreducible Representations of the Base Vectors in Space Group *Pnma* and Their Magnetic Symmetry Groups

representations[a]			magnetic (Shubnikov) group
G_x	C_y	A_z	*Pnma*
C_x	G_y	F_z	*Pn'm'a*
F_x	A_y	C_z	*Pnm'a'*
A_x	F_y	G_z	*Pn'ma'*

[a] For example, the antiferromagnetic zero-field structure of β-$CrAsO_4$ corresponds to G_z and so belongs to magnetic group *Pn'ma'*.

However, we have observed that α-$CrAsO_4$ decomposes to Cr_2O_3 and amorphous arsenic oxides over a period of months, suggesting that this is a metastable phase. This is further supported by the fact that β-$CrAsO_4$ does not transform to the α form upon heating below 900 °C and so is the thermodynamically stable polymorph at atmospheric pressure.

Chains of trans edge-shared CrO_6 octahedra oriented parallel with the *b* axis are the dominant structural feature of β-$CrAsO_4$. Each chromium–oxygen chain is linked to six other identical chains by sharing oxygen atom corners with AsO_4 tetrahedra (Figure 1). The bond distances and angles derived from the single-crystal structure determination show that the CrO_6 octahedra are very distorted, as was observed in β-$CrPO_4$. This is presumably due to the geometric constraints imposed by the structure, especially the edge-sharing of octahedra, as any deviation from regular octahedral coordination around t_{2g}^3 Cr^{3+} results in an unfavorable loss of ligand field stabilization energy. The atomic parameters obtained from the neutron powder experiment at 5 K are very similar to the room-temperature values, showing that there is no major structural distortion on cooling to this temperature. However, the percentage decreases in the cell parameters of β-$CrAsO_4$ on cooling from the paramagnetic state at room temperature to the magnetically ordered state at 5 K are 0.13 (7), 0.29 (12), and 0.14 (5) in *a*, *b*, and *c*, respectively; and as chains of octahedra lie parallel to *b*, resulting in strong antiferromagnetic interactions along this axis, the apparently large decrease in *b* may be due to these interactions (an exchange striction) as well as thermal contraction. It is also interesting to observe that the esd's on the oxygen parameters derived from the refinement using powder neutron data are smaller than those from the X-ray single-crystal analysis by a factor of 2–3. This illustrates the power of the former technique in determining the positions of light atoms.

The values of the magnetic moment and the Curie–Weiss temperature obtained from the high-temperature magnetic susceptibility data are consistent with a system of localized-electron $3d^3$ ($^4A_{2g}$) Cr^{3+} ions with antiferromagnetic interactions between the spins. This is in agreement with the magnetic structure determined from the neutron diffraction experiment, which shows that the moments are coupled antiferromagnetically along the chains of octahedra parallel to *b* and lie perpendicular to this axis as as result of dipole–dipole interactions. The interchain coupling of moments within the *ac* plane is also antiferromagnetic. The ordered magnetic moment of 2.38 (4) μ_B at 5 K is well below the ideal value of ~ 3 μ_B, which reflects significant covalency in the cation–anion interactions.[24]

However, the shift of the maximum in the magnetic susceptibility curve below T_N to higher temperatures with increasing field clearly indicates that there is an ordered ferromagnetic component, so that the overall behavior in an applied field is ferrimagnetic. This may reflect a ferromagnetic component that is too small to be detected in the neutron diffraction experiment, which was performed in the absence of a magnetic field, or the zero field state may be truly antiferromagnetic, in which case the weak ferromagnetism is entirely field-induced. The latter is only possible if the magnetic symmetry group of the crystal *permits* a ferromagnetic component in zero field, in addition to the antiferromagnetic state.[25] The overall spin configuration has to be

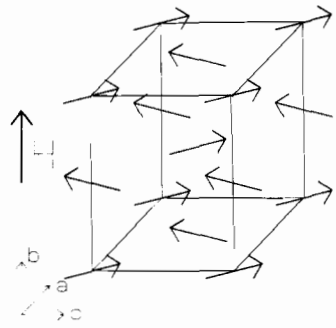

Figure 6. Proposed model for weak ferromagnetism in β-$CrAsO_4$ induced by a component of the applied magnetic field (*H*) in the direction of *b*. Moments are tilted away from *c* and lie in the *bc* plane.

invariant under the operations of the symmetry group, which limits the possible spin directions in the unit cell. The irreducible representations that arise are expressed in terms of the base vectors already given[22] and are shown in Table V. As the G_z spin configuration is observed, the magnetic symmetry group is *Pn'ma'* and so the only other allowed combinations are A_x and F_y. The latter mode describes a ferromagnetic component, which when combined with the G_z configuration produces the canted arrangement of moments shown in Figure 6. Thus, our observation that β-$CrAsO_4$ is antiferromagnetically ordered in the absence of a magnetic field, and yet behaves as a ferrimagnet in an applied field, is consistent with the magnetic symmetry, but we cannot discount the possibility that there is a weak ferromagnetic component in the zero-field state. Single-crystal susceptibility measurements would help to clarify the situation, but sufficiently large crystals have not yet been prepared. Recent work on a $CrVO_4$ type polymorph of $FePO_4$ has also provided evidence for antiferromagnetic behavior in zero field and weak ferromagnetism parallel to the chains of octahedra induced by an applied field at temperatures just below the Néel temperature.[15]

It is interesting to note that all the previously reported magnetic structures of $ZnSO_4$ type materials belong to magnetic group *Pnma*. Both $CuSO_4$[8] and $MnSeO_4$[9] have the A_z spin configuration in which antiferromagnetic ordering along the chains parallel to *b* is accompanied by ferromagnetic ordering in the perpendicular plane, while in β-$CoSO_4$ and $CoSeO_4$ all three allowed spin components in *Pnma*, as shown in Table V, are observed. The three spin configurations are antiferromagnetic, so field-induced ferrimagnetism is not possible without a change of magnetic symmetry. This has been demonstrated in magnetic susceptibility measurements on a single crystal of β-$CoSO_4$, in which a field-induced F_z component was reported,[25] presumably due to a spin-flop transition.

The origin of the differences between the magnetic structures of β-$CrAsO_4$ and $MnSeO_4$ or $CuSO_4$ must lie in the nature of the superexchange interactions between the chains of octahedra, which take place through Cr–O(*n*)–As–O(*m*)–Cr linkages (hereafter abbreviated to "*n,m* linkages", where *n* and *m* are the crystallographic labels used in Table II) as the chains are too far apart for direct Cr–Cr interactions to take place. In this structure, each spin is connected to those in the six neighboring chains by four such pathways per chain. For example, a spin at (0, 0, 0) is connected to those at ($^1/_2$, 0, $^1/_2$) and ($^1/_2$, $^1/_2$, $^1/_2$) by 1,2 linkages of equal length and to spins at ($^1/_2$, 0, $^1/_2$) and ($^1/_2$, $-^1/_2$, $^1/_2$) by 2,3 pathways. As the spins at ($^1/_2$, $\pm^1/_2$, $^1/_2$) are antiparallel to the spin at ($^1/_2$, 0, $^1/_2$), there is no apparent favorable alignment of the original spin with respect to the chain at ($^1/_2$, *y*, $^1/_2$) or those at ($-^1/_2$, *y*, $^1/_2$), etc. A similar argument applies to the chains at (0, *y*, ±1) as the (0, 0, 0) spin is connected by two 1,3 linkages to the spin at (0, 0, 1) and by one to each of the spins at (0, $^1/_2$, 1) and (0, $-^1/_2$, 1). Hence, there is no favorable direction for a spin to take with respect to those in the neighboring chains on consideration of the length and number of superexchange pathways alone. The same conclusion is reached for the $CrVO_4$ structure. The nature of the ordered magnetic structures in these MXO_4 compounds must then be determined by factors such as

(24) Tofield, B. C. *The Study of Covalency by Magnetic Neutron Scattering*; Spinger-Verlag: Berlin, Heidelberg, 1975; p 52.
(25) Krienes, N. M. *Sov. Phys.—JETP (Engl. Transl.)* **1961**, *13*, 534.

the geometry of the exchange pathways, the electronic structure and anisotropy of the M and X species, and the overlap of the different metal d orbitals with those on the XO_4 group. Clearly, these will be very sensitive to different M and X atoms, which accounts for the variety of magnetic structures seen in these compounds and the difficulty in rationalizing them.

Acknowledgment. The authors thank R. S. McLean for collecting the susceptibility data, M. W. Sweeten for technical assistance, and the SERC for the provision of neutron facilities and a studentship for J.P.A.

Registry No. Cr_2O_3, 1308-38-9; H_3AsO_4, 7778-39-4; β-$CrAsO_4$, 15070-22-1.

Supplementary Material Available: Table listing anisotropic thermal parameters (1 page); table of observed and calculated structure factors for β-$CrAsO_4$ (1 page). Ordering information is given on any current masthead page.

Contribution from the Department of Chemistry, Birkbeck College, University of London, London WC1E 7HX, U.K., and Department of Molecular Pharmacology, Smith Kline & French Laboratories, Philadelphia, Pennsylvania 19101

Copper(I) Complexes with Bidentate Tertiary Phosphine Ligands: Solution Chemistry and Antitumor Activity

Susan J. Berners-Price,[1a] Randall K. Johnson,[1b] Christopher K. Mirabelli,[1b] Leo F. Faucette,[1b] Francis L. McCabe,[1b] and Peter J. Sadler*[1a]

Received February 17, 1987

Copper may play an important role in the antitumor activity of diphosphines. The tetrahedral bischelated copper(I) complexes $[Cu(dppey)_2]Cl$ and $[Cu(dppp)_2]Cl$, where dppey is $Ph_2PCH{=}CHPPh_2$ and dppp is $Ph_2P(CH_2)_3PPh_2$, were synthesized and characterized. The bridged dicopper(I) complex $(CuCl)_2(dppe)_3$, where dppe is $Ph_2P(CH_2)_2PPh_2$, underwent dissociative equilibria in $CDCl_3$ and CD_2Cl_2 solutions, as determined by temperature-dependent ^1H and ^{31}P NMR studies. One of the products was $[Cu(dppe)_2]^+$, the proportion of which increased on adding excess dppe. The complex was also a product from the reaction of Cu^{2+} with excess dppe in DMA. The complexes $[Cu(P\text{-}P)_2]Cl$, where P-P is dppey or dppp, and $(CuCl)_2(dppe)_3$ were all active against P388 leukemia, M5076 reticulum cell sarcoma, and B16 melanoma. $[Cu(eppe)_2]Cl$, where eppe is $Et_2P(CH_2)_2PPh_2$, was active only against P388 leukemia. The activities were comparable to those of the analogous Au(I) complexes, and complexes were more potent than the free ligands.

Introduction

1,2-Bis(diphenylphosphino)ethane (dppe) and related phenyl-substituted diphosphines exhibit antitumor activity in several murine tumor models.[2] The activities of the bridged digold(I) complexes $XAu(Ph_2P(CH_2)_nPPh_2)AuX$, where X is for example Cl or thioglucose,[2] and tetrahedral bischelated Au(I) complexes $[Au(Ph_2P(CH_2)_nPPh_2)_2]X$, where X is e.g. Cl,[3,4] are comparable to those of the free ligands but the Au(I) complexes are 5- to 10-fold more potent.[2-4] The bridged digold complexes readily undergo ring-closure reactions to form chelated complexes. For example, the formation of $[Au(dppe)_2]^+$ from XAu(dppe)AuX (where X is Cl or thioglucose) occurs in the presence of thiols or blood plasma.[5] The antitumor activity of the diphosphines and the bridged complexes is highest for ligands that are able to form five- or six-membered chelate rings (i.e. n = 2, 3 or cis CH=CH).

Copper may play an important role in the mechanism of the cytotoxicity and antitumor activity. Cu(II) salts potentiate the cytotoxicity of diphosphines,[6] and $[Au(dppe)_2]Cl$ reacts in solution with Cu(II) to give a Cu(I) complex.[3] The aim of the present work was to synthesize tetrahedral copper(I) diphosphine complexes in the hope that these might exhibit pronounced activity.

There have been relatively few previous investigations of copper(I) diphosphine complexes. More effort has been directed toward monodentate tertiary phosphine complexes. These exhibit a wide variety of coordination geometries and stoichiometries[7] of the general formula $L_m(CuX)_n$, where L is a monophosphine and X an anion. The structures include monomeric, dimeric, and tetrameric species that often undergo complicated dissociative equilibria in solution involving species with different m:n stoichiometries.[8,9]

For the bidentate diphosphines, dppe and dppm complexes with P:Cu ratios of 4:1, 3:1, 2:1, 3:2, 4:3, and 1:1 have been isolated.[10-20] Some have been structurally characterized. They often contain both bridging halide and diphosphine ligands.[11-15] These complexes may dissociate in solution, but there have been no detailed studies of their solution chemistry. The stability of Cl–Cu–Cl linkages is particularly relevant to biological studies in view of the high concentration of Cl^- ions in, for example, blood plasma. With analogous gold complexes such bridges are rare.

The only known example of a copper(I) tetrakis(phosphine) complex with a halide counterion appeared to be $[Cu(PMe_3)_4]Cl$.[21] However, we were recently able to characterize $[Cu(eppe)_2]Cl$ (where $Ph_2P(CH_2)_2PEt_2$ is eppe) as a complex with remarkably high thermodynamic and kinetic stability, similar to the analogous bischelated Ag(I) and Au(I) complexes.[22] In the present work

(1) (a) Birkbeck College. (b) Smith Kline & French Laboratories.
(2) (a) Johnson, R. K.; Mirabelli, C. K.; Faucette, L. F.; McCabe, F. L.; Sutton, B. M.; Bryan, D. L.; Girard, G. R.; Hill, D. T. *Proc. Am. Assoc. Cancer Res.* **1985**, *26*, 254. (b) Mirabelli, C. K.; Hill, D. T.; Faucette, L. F.; McCabe, F. L.; Girard, G. R.; Bryan, D. B.; Sutton, B. M.; Bartus, J. O'L.; Crooke, S. T.; Johnson, R. K. *J. Med. Chem.*, in press.
(3) Berners-Price, S. J.; Mirabelli, C. K.; Johnson, R. K.; Mattern, M. R.; McCabe, F. L.; Faucette, L. F.; Sung, C.-M.; Mong, S.-M.; Sadler, P. J.; Crooke, S. T. *Cancer Res.* **1986**, *46*, 5486.
(4) Berners-Price, S. J.; Mirabelli, C. K.; Johnson, R. K.; Sadler, P. J., manuscript in preparation.
(5) Berners-Price, S. J.; Jarrett, P. S.; Sadler, P. J. *Inorg. Chem.*, in press.
(6) Snyder, R. M.; Mirabelli, C. K.; Johnson, R. K.; Sung, C.-M.; Faucette, L. F.; McCabe, F. L.; Zimmerman, J. P.; Whitman, M.; Hempel, J. C.; Crooke, S. T. *Cancer Res.* **1986**, *46*, 5054.
(7) Gill, J. T.; Mayerle, J. J.; Welcker, P. S.; Lewis, D. F.; Ucko, D. A.; Barton, D. J.; Stowens, D.; Lippard, S. J. *Inorg. Chem.* **1976**, *15*, 1155 and references cited therein.
(8) Lippard, S. J.; Mayerle, J. J. *Inorg. Chem.* **1972**, *11*, 753.
(9) Fife, D. J.; Moore, W. M.; Morse, K. W. *Inorg. Chem.* **1984**, *23*, 1684.
(10) Marsich, N.; Camus, A.; Cebulec, E. *J. Inorg. Nucl. Chem.* **1972**, *34*, 933.
(11) Albano, V. G.; Bellon, P. L.; Ciani, G. *J. Chem. Soc., Dalton Trans.* **1972**, 1938.
(12) Brescani, N.; Marsich, N.; Nardin, G.; Randaccio, L. *Inorg. Chim. Acta* **1974**, *10*, L5.
(13) Nardin, G.; Randaccio, L.; Zangrando, E. *J. Chem. Soc., Dalton Trans.* **1975**, 2566.
(14) Nardin, G.; Marsich, N.; Randaccio, L. *J. Am. Chem. Soc.* **1973**, *95*, 4053.
(15) Nardin, G.; Camus, A.; Randaccio, L. *Inorg. Chim. Acta* **1975**, *12*, 23.
(16) Edwards, D. A.; Richard, R. *J. Chem. Soc., Dalton Trans.* **1975**, 637.
(17) Anderson, W. A.; Carty, A. J.; Palenik, G. J.; Schreiber, G. *Can. J. Chem.* **1971**, *49*, 761.
(18) Gaughan, A. P.; Ziolo, R. F.; Dori, Z. *Inorg. Chem.* **1971**, *10*, 2776.
(19) (a) Dines, M. B. *Inorg. Chem.* **1972**, *11*, 2949. (b) Camus, A.; Marsich, N.; Nardin, G.; Randaccio, L. *Transition Met. Chem. (Weinheim, Ger.)* **1976**, *1*, 205.
(20) Leoni, P.; Pasquali, M.; Ghilardi, C. A. *J. Chem. Soc., Chem. Commun.* **1983**, 240.
(21) Schmidbauer, H.; Adlkofer, J.; Schwirter, K. *Chem. Ber.* **1972**, *105*, 3382.

0020-1669/87/1326-3383$01.50/0